Scheme II

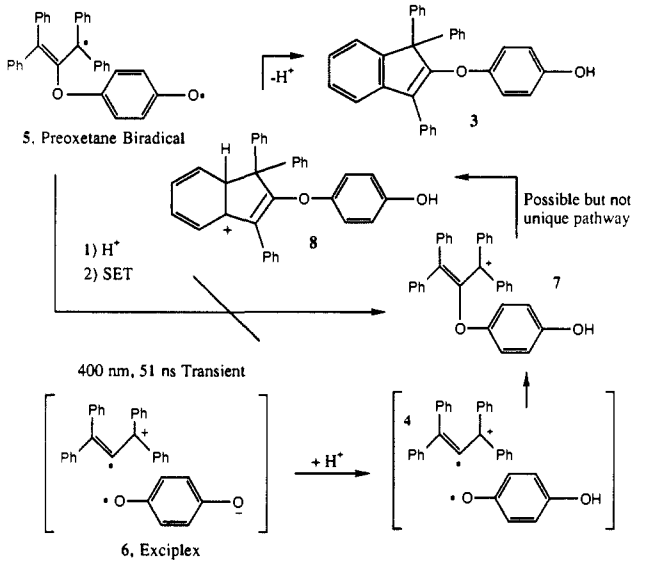


$AcOH/CCl_4$, drastic alterations in transient behavior are observed (Figure 1B, curve 1). In this case, decay of the initially formed 400-nm band [$(4.2 \pm 0.3) \times 10^7$ $s^{-1}$] and synchronous growth of the band at 610 nm [$(4.7 \pm 0.3) \times 10^7$ $s^{-1}$] are observed. The resulting three-maximum spectrum ($\lambda_{max}$ = 400, 490, and 610 nm) persisted for the duration of the experiment (1 $\mu$s). Both trifluoroacetic acid (TFA) and magic green[12,13] [MG, tris(2,4-dibromophenyl)aminium hexachloroantimonate] produce similar and, thus, apparently related three-maximum spectra (Figure 1C, $\lambda_{max}$ = 400, 475, and 590 nm) from TPA in the dark in $CCl_4$. In contrast, AcOH fails to afford a similar spectrum in the dark. While no rigorous assignments can be made for the species that afford the spectra in Figure 1, parts B and C, the strong similarities in these spectra indicate that the photochemical transient (Figure 1B, curve 1) is derived from electrophilic attack on the TPA.[14]

The preoxetane biradical **5** (Scheme II) was excluded as the initially observed transient (Figure 1A), since there is no obvious reason why **5** should be prone to rapid protonation under such mild conditions. Instead, a charge-transfer exciplex **6** would seem to be the more likely structure for this prompt transient. Protonation of the basic PBQ radical anion moiety should lead to a neutral semiquinone radical, which can couple with the TPA moiety at its central carbon atom either within a cage or following diffusion. The exact sequence of events leading from exciplex **6** to the product **3** is not clear; acid-assisted coupling of the PBQ and TPA moieties may precede cyclization to the indene skeleton as illustrated in Scheme II, or alternatively, cyclization may precede coupling. Furthermore, the bands of the long-lived transient spectrum (Figure 1B, curve 1) might be due to some combination of the open cation **7**, the cyclized cation **8**, or other closely related species. The tentative mechanism outlined in Scheme II is supported by the previous observation of reactions of CT exciplexes with Brönsted[2c] and Lewis acids,[15] as well as salt effects in Paterno-Büchi reactions.[3g] Finally, this photochemical cyclization to **3** closely parallels the efficient, thermal cyclization of TPA to 1,1,3-triphenylindene in TFA.

In summary, this work provides transient spectroscopic evidence for exciplex intermediacy in at least one photoreaction of a carbonyl compound with an olefin. Additional work directed toward the interception of related exciplexes with acids should further characterize these carbonyl-olefin intermediates and probably lead to novel chemistry as well.

**Acknowledgment.** K.A.S. thanks the University of Cincinnati Summer Research Council, the Procter & Gamble Company, the Research Associates Program, and the Center for Laser Chemistry for stipend support. We thank the National Science Foundation for partial support of this work (R.M.W., CHE-8312691 and CHE-8409628; R.A.C., CHE-8516534 and CHE-8820268). Kinetic absorption spectroscopy was performed at the Center for Fast Kinetic Research at the University of Texas at Austin, supported by NIH Grant RR-00886 from the Biotechnology Branch of the Division of Research Resources and by the University of Texas.

**Registry No. 3**, 126035-47-0; **6**, 126035-49-2; *p*-benzoquinone, 106-51-4; *p*-benzoquinone radical anion, 3225-29-4; tetraphenylallene, 1674-18-6; tetraphenylallene radical anion, 126035-48-1; 2-methoxy-1,1,3-triphenylindene, 126035-50-5; 3-methoxy-1,1',3,3'-tetraphenylpropene, 86477-15-8; 2-(4-(4-bromobenzoyloxy)phenoxy-1,1,3-triphenylindene, 126035-51-6.

**Supplementary Material Available:** Figure showing the atomic numbering scheme, X-ray experimental description, X-ray structure determination summary, and X-ray data tables for the *p*-bromobenzoate derivative of **3**, including Table 3-1 of atomic positional parameters, Table 3-2 of anisotropic temperature factors, Table 3-3 of hydrogen positional parameters, Table 3-4 of bond distances, and Table 3-5 of bond angles (13 pages). Ordering information is given on any current masthead page.

## Immobilizing the Gate of a Tartaric Acid–Gramicidin A Hybrid Channel Molecule by Rational Design

Charles J. Stankovic, Stefan H. Heinemann,*,† and Stuart L. Schreiber*,‡

*Department of Chemistry, Harvard University 12 Oxford Street, Cambridge, Massachusetts 02138 Max-Planck-Institut für Biophysikalische Chemie Abteilung Membranbiophysik, Am Fassberg D-3400 Göttingen, FRG*

*Received January 16, 1990*

The ability to control the gating of ion-conducting channel molecules represents an important step toward the goal of producing molecular switches. Recently we developed a transmembrane ion channel motif based on tartaric acid–gramicidin A hybrids.[1,2] By covalent linkage of two gramicidin A (gA) monomers, the problem of channel disruption seen in the native channel can be removed.[3] Single-channel ion conductance measurements of **1** and **2** (Figure 1) demonstrated that the ion-conducting properties of these molecules are dependent on the stereochemistry of the tartaric acid derived linker element, in accord with the predictions of a structural model based on a $\beta$-helix secondary structure. In this model, the *S,S* stereochemistry of the dioxolane is matched with respect to the helix geometry, whereas the (*R,R*)-dioxolane linker is a stereochemical mismatch. Importantly, it was noted that diastereomer **2** exhibited rapid interruptions in current (flickers), a property suggestive of a gating mechanism. A structural basis for the diastereospecific gating was proposed that involves the movement of the dioxolane ring in **2** into and out of the ion-conducting pore, resulting in the closed and open form of the channel. A prediction of this model is that the introduction of sterically demanding substituents at the acetal

(12) Bell, F. A.; Ledwith, A.; Sherrington, D. C. *J. Chem. Soc. C* **1969**, 2719.

(13) Wilson, R. M.; Dietz, J. G.; Shepherd, T. A.; Ho, D. M.; Schnapp, K. A.; Elder, R. C.; Watkins, J. W., II; Geraci, L. S.; Campana, C. F. *J. Am. Chem. Soc.* **1989**, *111*, 1749.

(14) Presumably the spectrum of the photochemical transient (Figure 1B, curve 1) is shifted to slightly longer wavelength by the hydroquinone substituent.

(15) Bowman, R. M.; Chamberlain, T. R.; Huang, C. W.; McCullough, J. J. *J. Am. Chem. Soc.* **1970**, *92*, 4106.

* To whom correspondence should be addressed.
† Max-Planck-Institut für Biophysikalische Chemie.
‡ Harvard University.

(1) Heinemann, S. H.; Stankovic, C. J.; Delfino, J. M.; Schreiber, S. L.; Sigworth, F. J. *Biophys. J.* **1989**, *55*, 505a.

(2) Stankovic, C. J.; Heinemann, S. H.; Delfino, J. M.; Sigworth, F. J.; Schreiber, S. L. *Science* **1989**, *244*, 813-817.

(3) (a) Urry, D. W.; Goodall, M. C.; Glickson, J. D.; Mayers, D. F. *Proc. Natl. Acad. Sci. U.S.A.* **1971**, *68*, 1907-1911. (b) Bamberg, E.; Janko, K. *Biochim. Biophys. Acta* **1977**, *465*, 486-499.

0002-7863/90/1512-3702$02.50/0 

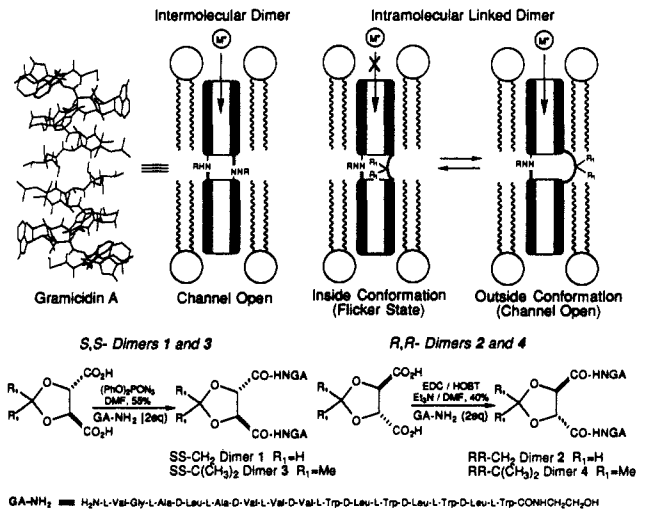


**Figure 1.**

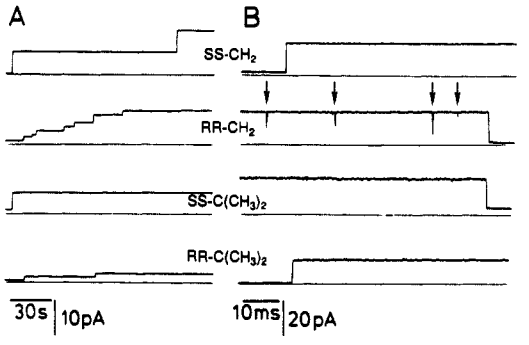


**Figure 2.** (A) Current traces recorded for SS-$CH_2$ **1**, RR-$CH_2$ **2**, SS-$C(CH_3)_2$ **3**, and RR-$C(CH_3)_2$ **4** (from GMO/squalene membranes in symmetrical 640 mM KCl solutions at 200 mV membrane potential) indicating the long lifetime of these covalently linked channels and the difference in conductance between the *S,S* and *R,R* isomers. (B) Short sections of single-channel current events at a faster time scale in the same order as in A in 40 mM HCl and 200 mV. Note that the single-channel conductance for protons is essentially equal for all compounds. Only in RR-$CH_2$ **2** are brief current interruptions observed (see arrows). The same flickering behavior is observed in KCl solutions. The corresponding current in natural gA would be 15.2 pA.

carbon of the dioxolane ring of **2** should inhibit this conformational dynamism and, accordingly, abolish the gating phenomenon. Herein we report a synthesis of dimethyl-substituted analogues of **1** and **2** (i.e., **3** and **4**) and a single-channel high-resolution analysis of their ion-conducting properties.

The flickers seen in the single-channel conductance data for **2** with alkali ions also occur for proton fluxes and always represent conformational states of vanishing conductance (see Figures 2 and 3). The rate of flickering for **2** was 100 $s^{-1}$, and the dwell time in the flicker (closed) state was 71 $\mu$s at 21 °C, causing the channel to be closed for approximately 1% of the time. No such flickering was observed for diastereomer **1**. The dimensions of the pore formed by the channel molecules are sufficient to support only a single column of 8–12 water molecules that form a continuous hydrogen-bonded chain from one end of the channel to the other. Most cations must pass through the channel in single file, pushing the column of water molecules along in front of them. On the other hand, proton flux through the channel can occur via a proton relay process involving the resident water molecules (Grotthus mechanism[4]). This process allows proton fluxes 10–100 times higher than those observed for other ions. The observation that the conductance of protons in the flicker state drops to 0 supports our hypothesis that a severe steric blockage of the channel has occurred, so that even the hydrogen-bonding network has been disrupted.

(4) Levitt, D. G. *Biophys. J.* **1978**, *22*, 209–248.

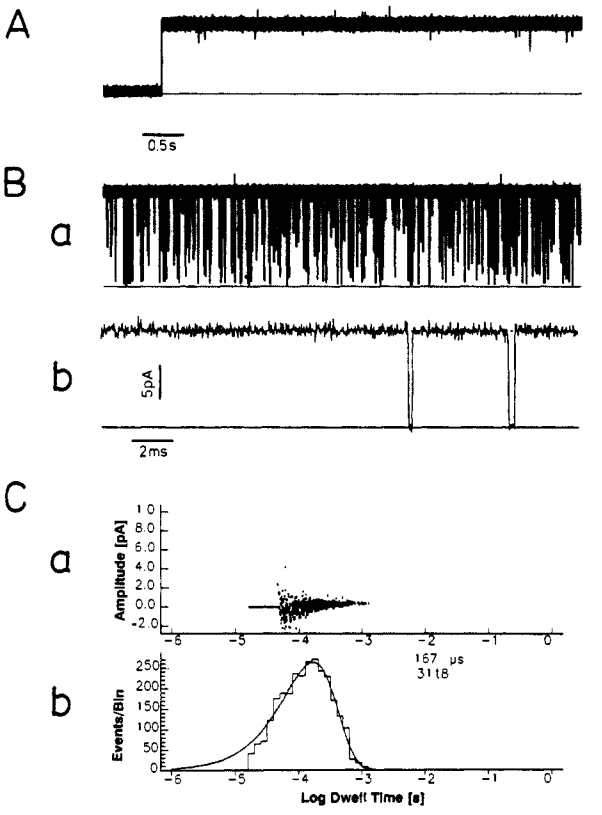


**Figure 3.** Comparison of current recordings from (A) RR-$C(CH_3)_2$ **4** and (B) (a) RR-$CH_2$ **2** (GMO/squalene, symmetrical 40 mM HCl solutions, 200 mV membrane potential, 20.0 °C and 15.3 °C, respectively), showing the high density of flickers in **2** relative to **4**. (b) Section of trace a on an expanded time scale. It is clearly seen that the current interruptions reach the base line, i.e., they are complete channel closures. (C) Current scatter plot (top) and dwell time histogram (bottom) of the closing events in logarithmic time scaling. A single-exponential curve corresponding to a mean closed time of 167 (±3) $\mu$s is superimposed. The frequency of occurrence of the channel flickers was 18 (±1) $s^{-1}$ ($N$ = 3118).

The rate and dwell time of the flickers indicate that the flicker state is both kinetically and thermodynamically disfavored (relative to the open-channel state) in **2**, while the results for the SS-$CH_2$ dimer **1** indicate that even minor changes in the structure of the linker can completely eliminate this phenomenon. In the latter diastereomer, the linker is a stereochemical match with the helix geometry when placed outside of the channel.[1,2] The addition of two methyl groups to the acetal carbon of the linker should not only decrease the stability of the ring inside the pore, causing a decrease in the dwell time (Figure 4), but also increase the barrier to ring flipping as the methyls would suffer steric crowding as the linker swings through the next turn of the helix.

To test this prediction, the transmembrane channel molecules **3** and **4** were synthesized[5] and their ion conductance properties were assayed after incorporation into artificial lipid bilayers.[6,7] Figures 2 and 3 show typical current traces for each of these

(5) These dimers were prepared in analogy to the previously reported method (ref 2). The $^1H$ NMR, UV, and mass spectra were fully consistent with the assigned structures.

(6) Sigworth, F. J.; Urry, D. W.; Prasad, K. *Biophys. J.* **1987**, *52*, 1055–1064.

(7) Experiments were carried out in symmetrical unbuffered salines of either 640 mM KCl (pH 6.0) or 40 mM HCl (pH 1.9) and used glycerol monooleate (GMO, Nu Check Prep., Elysian, MN), 40 mg/mL in squalene (Sigma, St. Louis, MO), as the lipid component. Bilayers were formed on patch-clamp pipet tips of 3–5-$\mu$m diameter. Current data, recorded with a commercial patch-clamp amplifier (EPC7, List Medical, Darmstadt, FRG), were stored in digital form on videotape. Further data processing was performed on a VME-bus based laboratory computer system (Motorola MVME147, Tempe, AZ). The gramicidin samples were stored in methanolic stock solutions at −20 °C. Approximately 1 $\mu$L of 10 ng/mL gramicidin was then added to the 1.5 mL of the lipid/solvent mixture before membranes were formed.

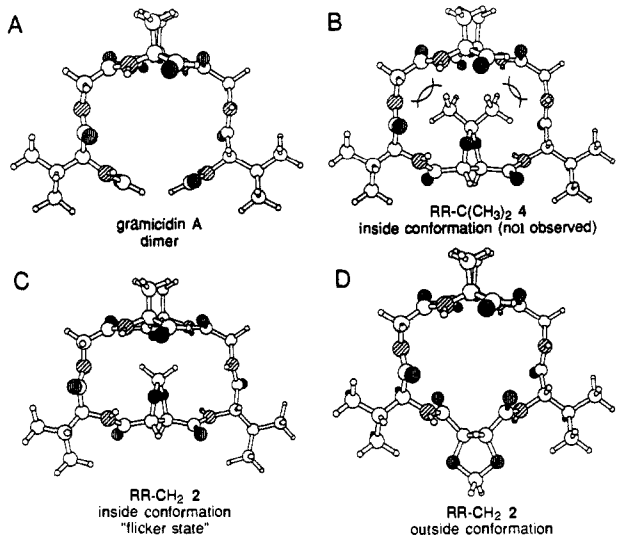


Figure 4. Top view through the central turn of the channel helix including the linker (for comparison, natural gA is also shown): (A) natural gA with no linker, (D) the linker ring of **2** outside and (C) inside the pore. The bulkier ring of **4** cannot be accommodated inside the channel pore (B) and suffers severe steric strain in the inside–outside transition (diagram not provided).

dimers. Note that each upward rise indicates a channel opening and represents the ion flux through a *single molecule* of the dimer. Each dimer exhibited very long open-channel lifetimes (>30 min). Under identical conditions, gA channels have a lifetime of 10–120 s. Both *S,S* dimers **1** and **3** have conductances similar to that of gA, whereas the conductances of the *R,R* dimers **2** and **4** in KCl (Figure 2A) are lower than those of the *S,S* dimers. In HCl solutions the conductances of all the dimers, as well as of gA, are nearly the same (Figure 2B). These latter observations are readily explained by the Grotthus mechanism of proton conductance mentioned above. While proton conductance is sensitive to a complete blockage of the channel, it is not very sensitive to structural distortions along the channel as long as the water chain inside the channel remains intact. The conductance of alkali ions, however, is expected to be susceptible to even minor steric disturbances, due to the attendant effect on the solvation of the ion as it passes through the channel. Whereas both *S,S* dimers exhibit a linear current–voltage (*iV*) relationship, both *R,R* (mismatched) dimers exhibit a hyperlinear current–voltage relationship (data not shown). These results also indicate that the *R,R* dimers have a disturbance at the center of the channel.[8]

A clear distinction between the *R,R* dimers **2** and **4** can be seen in the traces shown in Figure 2B. The RR-$C(CH_3)_2$ dimer **4** does not exhibit the flickering behavior found in the RR-$CH_2$ dimer **2** (Figure 3). This result provides support for our hypothesis that the flickers are caused by the flipping of the dioxolane ring of **2** into and out of the channel since the dioxolane ring in the RR-$C(CH_3)_2$ dimer **4** is expected to be too large to either fit inside the channel (see Figure 4) or undergo the inside–outside transition. This study represents one step toward a detailed understanding of the dynamic properties of artificial channel molecules such as **2**. An increased understanding of gating mechanisms is hoped to facilitate the rational design of control elements for the gating of transmembrane ion channels.[9]

**Acknowledgment.** S.H.H. was supported by a stipend of the Max-Planck-Gesellschaft. S.L.S. is pleased to acknowledge the NIGMS for generous support and Pfizer, Inc., for a graduate fellowship (awarded to C.J.S.). We thank Professor M. Karplus and B. Roux for the coordinates of the gA helix dimers, Dr. G. Glick and B. Roux for helpful suggestions regarding molecular modeling, Professors E. Neher and F. J. Sigworth for support of S.H.H., and Dr. W. McMurray (Mass Spectrometry Facility at the Yale Comprehensive Cancer Center).

(8) This conclusion is based on a formalism describing the ion transport by migration of ions through an energy profile with two minima and three barriers. See ref 2.

(9) See also: (A) Lear, J. D.; Wasserman, Z. R.; DeGrado, W. F. *Science* **1988**, *240*, 1177. (b) Carmicheal, V. E.; Dutton, P. J.; Fyles, T. M.; James, T. D.; Swan, J. A.; Zojaji, M. *J. Am. Chem. Soc.* **1989**, *111*, 767. (c) Jullien, L.; Lehn, J.-M. *Tetrahedron Lett.* **1988**, *29*, 3803 and references therein.

## Phospholipase $A_2$ Engineering. 3. Replacement of Lysine-56 by Neutral Residues Improves Catalytic Potency Significantly, Alters Substrate Specificity, and Clarifies the Mechanism of Interfacial Recognition[1]

Joseph P. Noel, Tiliang Deng, Kelly J. Hamilton, and Ming-Daw Tsai*

*Department of Chemistry and Biochemistry Program*
*The Ohio State University, Columbus, Ohio 43210*
*Received January 17, 1990*

We report substantial improvement in the catalytic potency of *bovine* pancreatic phospholipase $A_2$ (PLA2, overexpressed in *Escherichia coli*)[2,3] toward natural substrate phosphatidylcholine (PC) when Lys-56 was replaced by neutral amino acids, particularly methionine. As shown by the kinetic data summarized in Table I, the methionine mutant (K56M) shows a 4–5-fold increase in $k_{cat}$ and a 4–5-fold decrease in $K_m$, and as a consequence, a 20–25-fold increase in $k_{cat}/K_m$ for micellar dioctanoyl-PC ($DC_8PC$) and diheptanoyl-PC ($DC_7PC$) and monomeric dihexanoyl-PC ($DC_6PC$) and $DC_7PC$. Replacement of Lys-56 by other neutral amino acids Asn and Thr (K56N and K56T, respectively) also resulted in increased $k_{cat}$ and decreased $K_m$, but to a smaller extent. Mutation to the positively charged Arg (K56R) resulted in very small changes.

Most, if not all, of the reported increases in $k_{cat}/K_m$ for site-specific mutants were either for partial reactions or substrate analogues with lower activity (actually a change in substrate specificity).[4] The increase in $k_{cat}/K_m$ for the K56M mutant should represent improved catalytic potency and is the largest reported to date, since $DC_8PC$ micelle is the best natural substrate of bovine pancreatic PLA2. The highest $k_{cat}$ observed for *bovine* K56M is even higher than that of the anionic substrate analogue $DC_8$-sulfate known to activate *porcine* PLA2.[5] Both $k_{cat}$ and $k_{cat}/K_m$ of K56M are comparable to those of dimeric snake venom PLA2 (Thr at position 56)[6] for $DC_8PC$ micelles and are significantly higher for $DC_6PC$ monomers[7] (see the last three rows of Table I). Crystal structural analysis by Sigler[6] suggested that one of the main causes for the higher catalytic efficiency of snake venom PLA2 is that the loop 57–66 (absent in dimeric snake venom enzymes) prevents the pancreatic enzyme from dimerization.[7] Recently Kuipers et al.[8] reported that deletion of this loop (Δ62–66) from *porcine* pancreatic PLA2 did result in en-

(1) For papers 1 and 2 in this series, see refs 2 and 3, respectively. This work was supported by Research Grant GM41788 from NIH. We thank Dr. R. L. Heinrikson for sharing the results in ref 11 prior to publication.

(2) Noel, J. P.; Tsai, M.-D. *J. Cell. Biochem.* **1989**, *40*, 309–320.

(3) Deng, T.; Noel, J. P.; Tsai, M.-D., submitted to *Gene*.

(4) (a) Takagi, H.; Morinaga, Y.; Ikemura, H.; Inouye, M. *J. Biol. Chem.* **1988**, *263*, 19592–19596. (b) Wilkinson, A. J.; Fersht, A. R.; Blow, D. M.; Carter, P.; Winter, G. *Nature* **1984**, *307*, 187–188. (c) Estell, D. A.; Graycar, T. P.; Miller, J. V.; Powers, D. B.; Burnier, J. P.; Ng, P. G.; Wells, J. A. *Science* **1986**, *233*, 659–663. (d) Wells, J. A.; Cunningham, B. C.; Graycar, T. P.; Estell, D. A. *Proc. Natl. Acad. Sci. U.S.A.* **1987**, *84*, 5167–5171. (e) Bone, R.; Silen, J. L.; Agard, D. A. *Nature* **1989**, *339*, 191–195.

(5) (a) Van Oort, M. G.; Dijkman, R.; Hille, J. D. R.; de Haas, G. H. *Biochemistry* **1985**, *24*, 7993–7999. (b) Volwerk, J. J.; Jost, P. C.; de Haas, G. H.; Griffith, O. H. *Biochemistry* **1986**, *25*, 1726–1733.

(6) Renetseder, R.; Brunie, S.; Dijkstra, B. W.; Drenth, J.; Sigler, P. B. *J. Biol. Chem.* **1985**, *260*, 11627–11634.

(7) Wells, M. A. *Biochemistry* **1974**, *13*, 2248–2257.

(8) Kuipers, O. P.; Thunnissen, M. G. G. M.; de Geus, P.; Dijkstra, B. W.; Drenth, J.; Verheij, H. M.; de Haas, G. H. *Science* **1989**, *244*, 82–85. Unlike $DC_8PC$, the $k_{cat}/K_m$ for micellar $DC_7PC$ is comparable between their deletion mutant and our K56M. Thus the effect of porcine Δ62–66 is more on altering substrate specificity.

0002-7863/90/1512-3704$02.50/0 